Electrochimica Acta 263 (2018) 237–248

Contents lists available at ScienceDirect

Electrochimica Acta

journal homepage: www.elsevier.com/locate/electacta

Effects of the $LiPO_2F_2$ additive on unwanted lithium plating in lithium-ion cells

Q.Q. Liu [a, b], Lin Ma [c], C.Y. Du [a, **], J.R. Dahn [b, c, *]

[a] MIIT Key Laboratory of Critical Materials Technology for New Energy Conversion and Storage, School of Chemistry and Chemical Engineering, Harbin Institute of Technology, Harbin, 150001, China
[b] Dept. of Physics and Atmospheric Science, Dalhousie University, Halifax, N.S. B3H4R2, Canada
[c] Dept. of Chemistry, Dalhousie University, Halifax, N.S. B3H4R2, Canada

ARTICLE INFO

Article history:
Received 18 November 2017
Received in revised form
28 December 2017
Accepted 9 January 2018
Available online 10 January 2018

ABSTRACT

The effect of the additive lithium difluorophosphate ($LiPO_2F_2$) on unwanted lithium plating in lithium-ion cells was studied in this work. $Li[Ni_{1/3}Mn_{1/3}Co_{1/3}]O_2$/graphite pouch cells were cycled at high charge rates where unwanted lithium plating was identified as the major aging mechanism. $LiPO_2F_2$ used as a single electrolyte additive reduced cell impedance growth during cycling even at high charge rate (i.e. 2C) at 20 °C. Electrochemical impedance spectroscopy (EIS) measurements on symmetric cells showed that $LiPO_2F_2$ reduced the growth of both positive and negative electrode impedances during cycling. The effects of $LiPO_2F_2$ depend strongly on the presence of other additives. When $LiPO_2F_2$ was combined with 2% propene sultone (PES) + 1% ethylene sulfate (DTD) + 1% tris(-trimethyl-silyl)-phosphite (TTSPi) (called PES211), the cell impedance increased which led to unwanted lithium plating. When 1% $LiPO_2F_2$ was used in combination with ethylene sulfate (DTD) or fluoroethylene carbonate (FEC) the impedance of the cells grew more slowly with cycling than with DTD or FEC added alone. Normally, but not always, additions of $LiPO_2F_2$ reduce cell impedance. The choice of additives to use along with $LiPO_2F_2$ must be made wisely to ensure synergistic action.

© 2018 Elsevier Ltd. All rights reserved.

1. Introduction

Reducing the time to charge Li-ion cells is desired for both portable electronics and electric vehicle applications. The main impediment to high charge rates is the proximity of the potential of lithiated graphite (+0.08 V vs. Li/Li^+) to that of lithium metal (0.0 V vs. Li/Li^+), when $½ < x < 1$ in Li_xC_6. Sufficient polarization in the cell can drive the graphite potential below the lithium potential and then unwanted Li plating will occur. This deposited lithium has a negative impact on the lifetime of Li-ion cells and unwanted lithium plating is therefore the dominant aging mechanism when high charge rates and/or low temperatures are applied to lithium ion cells [1–3].

The propensity for unwanted lithium plating strongly depends on parameters that increase the polarization of the graphite electrode such as harsh charging conditions (e.g., high charge rates, low temperatures) [4], thick electrodes [5], low Li-ion diffusion constant or large graphite particle size [6,7] and a highly-resistive solid electrolyte interphase (SEI) [8,9]. Among these, the SEI of the graphite electrode, which is controlled by the electrolyte components, strongly influences the negative electrode impedance [1] and strongly affects unwanted lithium plating at high charge rates. Many electrolyte additives that promote longer lifetime Li-ion cells lead to negative electrodes with high resistance and unfortunately limit the charging rates of cells due to unwanted lithium plating [9]. John-Paul Jones et al. [8] found that electrolyte additives such as vinylene carbonate (VC), lithium bis(oxalato) borate (LiBOB) and 3-propane sultone (PS) increased the negative electrode resistance and thus increased the propensity for lithium plating. Therefore, in order to improve the fast-charge capability of graphite electrode, the electrolyte additives used should form a less-resistive SEI.

Lithium difluorophosphate ($LiPO_2F_2$) is a very promising electrolyte additive that could improve high-temperature storage which will be shown in Fig. 1. In addition, it was reported that $LiPO_2F_2$ as a single additive improved the discharge performance at

* Corresponding author. Dept. of Chemistry, Dalhousie University, Halifax, N.S. B3H4R2, Canada.
** Corresponding author.
E-mail addresses: cydu@hit.edu.cn (C.Y. Du), jeff.dahn@dal.ca (J.R. Dahn).

https://doi.org/10.1016/j.electacta.2018.01.058
0013-4686/© 2018 Elsevier Ltd. All rights reserved.

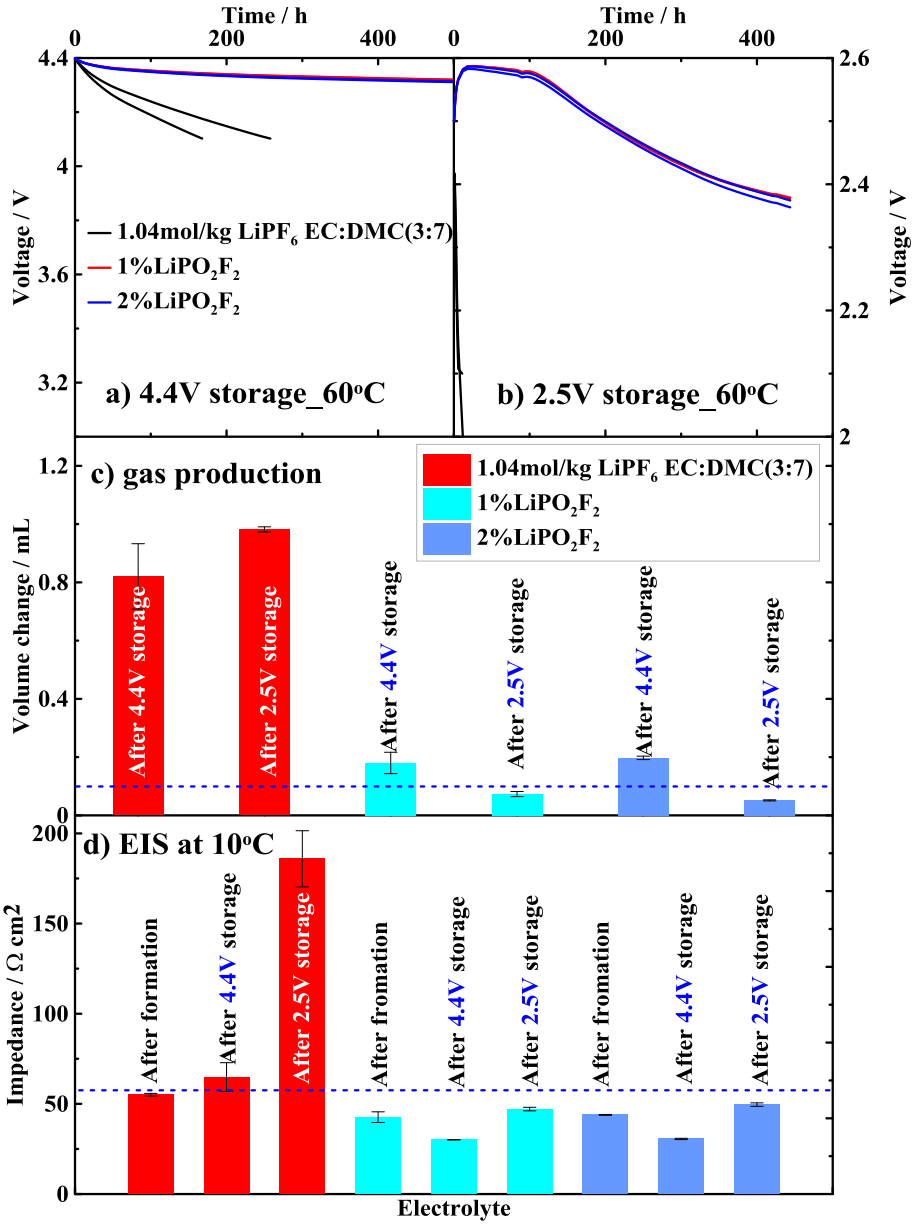

Fig. 1. Open circuit voltage versus time during storage at 60 °C: a) 4.4 V and b) 2.5 V, for 500 h for NMC532/graphite pouch cells containing 1.04 mol/kg $LiPF_6$ EC:DMC (3:7) with 1% $LiPO_2F_2$ or 2% $LiPO_2F_2$; c) gas volumes generated during the 60 °C storage periods at 4.4 V and 2.5 V and d) summary of R_{ct} (diameter of the semi-circle in the EIS spectrum) for NMC532/graphite pouch cells containing 1.04 mol/kg $LiPF_6$ EC:DMC (3:7) with 1% $LiPO_2F_2$ or 2% $LiPO_2F_2$. Two cells were measured for each data point and the error bars in c) and d) are the difference between the two results.

low temperatures [10,11] and $LiPO_2F_2$ combined with VC enhanced the rate capability of graphite/Li coin cells [12]. Therefore, $LiPO_2F_2$ should hinder unwanted lithium plating.

In addition to $LiPO_2F_2$ alone, other additives should be considered in combination with it. Ethylene sulfate (DTD) was reported to form a suitable SEI on the graphite electrode so that it could operate in PC-containing electrolytes [13,14]. Sano and Maruyama also showed that cells containing DTD provided relatively good rate capability [15]. In addition, FEC can facilitate SEI formation through preferential reduction on the graphite surface and improve the low-temperature performance of graphite/Li coin cells [16,17].

In this paper, electrolyte additives that create low SEI resistance were chosen to study their effects on unwanted lithium plating in Li $[Ni_{1/3}Mn_{1/3}Co_{1/3}]O_2$ (NMC111)/graphite pouch cells during cycling at high rates and/or low temperatures. The electrolyte additives used include: $LiPO_2F_2$ and the combinations of 1% $LiPO_2F_2$ with 2% VC, PES211, 2% FEC and 1% DTD. The additives 2% VC [18,19] and PES211 [20,21] are very effective for improving cell lifetime but yield relatively high impedance. $LiPO_2F_2$ was combined with 2% VC or PES211 to see if the additives acted synergistically to yield both high-rate and long lifetime Li ion cells. Charge-discharge cycling of NMC111/graphite pouch cells at 20 °C with different charge rates was used to determine the onset current for unwanted lithium plating. Increased capacity loss with cycle number was used to detect unwanted lithium plating. Electrochemical impedance spectroscopy (EIS) measurements were used on the full pouch cells, negative electrode symmetric cells and positive electrode symmetric cells to investigate how the charge transfer resistances of the negative electrodes affected unwanted lithium plating.

2. Experimental

1 M $LiPF_6$ (BASF, purity 99.94%) in EC:EMC (3:7 wt% ratio, BASF, purity 99.99%) was used as the control electrolyte. To the control electrolyte, $LiPO_2F_2$ (Shenzhen Capchem Technology Co., China or Guangzhou Tinci New Materials Technology Co., China) was added as an additive at 1 or 2 wt % (note that 2% $LiPO_2F_2$ was not fully dissolved). The electrolyte additives PES211 (PES: Lianchuang Medicinal Chemistry Co., Ltd., China, purity 98.20%; TTSPi: TCI America, purity > 95%; DTD: Sigma Aldrich, purity 98%), 2 wt % VC (purity > 99.8%, BASF), 2 wt % FEC (BASF, purity 99.94%) and 1% wt. DTD, added singly or in combination with 1% $LiPO_2F_2$ to the control electrolyte, were also studied.

The pouch cells used in this study were NMC111/graphite cells with a capacity of 220 mAh (balanced for 4.4 V) with a negative/positive capacity ratio of about 1.17 at 4.1 V. Cells were manufactured by Li-Fun Technology (Xinma Industry Zone, Golden Dragon Road, Tianyuan District, Zhuzhou City, Hunan Province, PRC, 412000) and vacuum sealed without electrolyte before shipping to our laboratory in Canada. The pouch cells are 40 mm long x 20 mm wide x 3.5 mm thick. The detailed information about the positive and negative electrode materials in these NMC111/graphite pouch cells are given in Refs. [9,22]. All cells were cut open and vacuum dried at 100 °C for 14 h before electrolyte filling. Then cells were transferred immediately to an argon-filled glove box for electrolyte filling and vacuum sealing. The pouch cells were filled with 0.76 mL (about 0.90 g) of electrolyte. After filling, cells were vacuum-sealed with a compact vacuum sealer (MSK-115A, MTI Corp.).

The formation process for the cells was as follows. First, the pouch cells were held at 1.5 V for 24 h to ensure complete wetting of the electrolyte with the electrodes and separator. After wetting, cells were charged to 3.5 V at 11 mA (C/20) and held at 3.5 V for 1 h (all at 40 °C). Then the cells were cut open to release gas and vacuum sealed again in the argon-filled glovebox. After degassing, these cells were charged to 4.1 V and discharged to 3.8 V at C/20 and 40 °C, then held at 3.8 V for 1 h to prepare them for EIS measurements.

EIS measurements were conducted on NMC111/graphite pouch cells both after formation and after cell cycling. Prior to EIS measurement, cells were charged or discharged to 3.8 V and held for 1 h to stabilize cell voltage. A voltage of 3.8 V was chosen because both graphite and NMC electrodes are at about 50% state of charge at this voltage. All EIS spectra were measured using a Biologic VMP3 electrochemical test station. Data were collected with ten points per decade from 100 kHz to 10 mHz with a signal amplitude of 10 mV.

After EIS measurements, the cells were charged and discharged with constant currents (C-rates) of 110 mA (C/2), 220 mA (1C), 330 mA (1.5C) or 440 mA (2.0C) between 2.8 and 4.1 V using a Maccor charger system at 20. ± 0.1 °C. Pair cells were tested for every charge rate to ensure reproducibility. In order to determine the active lithium loss during cycling, cells were cycled at C/20 one time before and after the high charge rate segments. The upper cutoff voltage was set to 4.1 V in order to minimize electrolyte oxidation at the positive electrode and to ensure that the cells were far from having a fully loaded negative electrode which would occur at 4.4 V for these cells. All pouch cells were cycled with external clamps to eliminate effects of small amounts of gas that

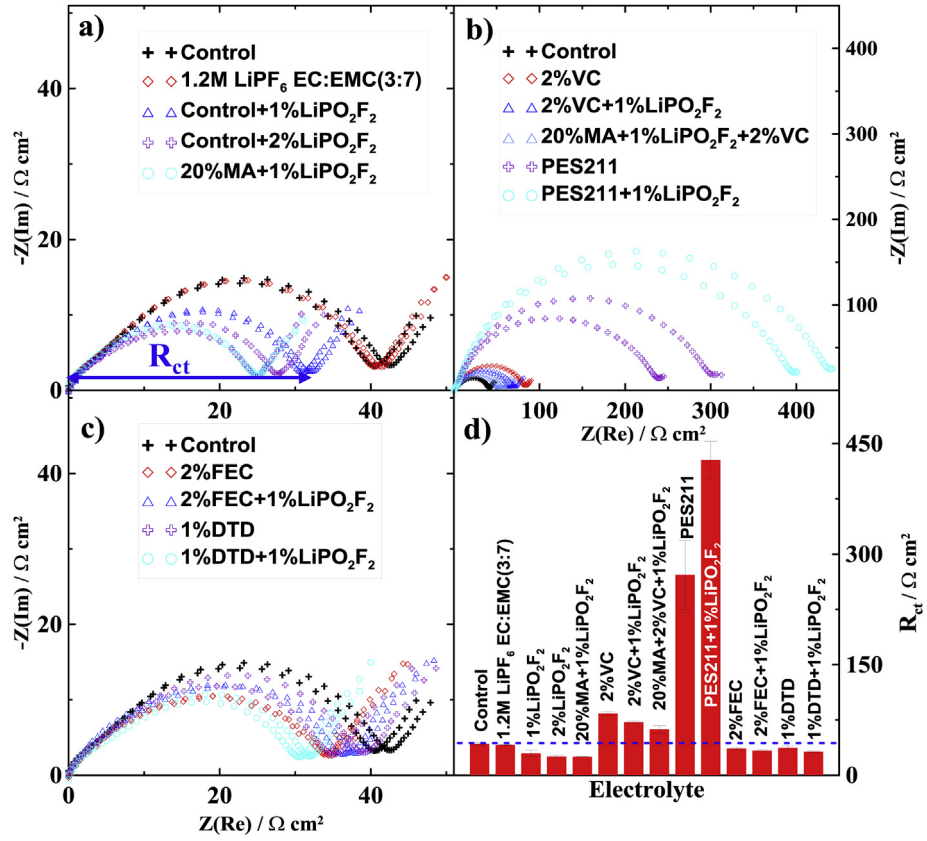

Fig. 2. Impedance spectra measured at 3.8 V and 10. ± 0.1 °C of NMC111/graphite pouch cells with: (a) control, control + 1% $LiPO_2F_2$, control + 2% $LiPO_2F_2$, 1.2 M $LiPF_6$ in EC:EMC (3:7), 1.2 M $LiPF_6$ in [20% MA+ 80% EC:EMC (3:7)] + 1% $LiPO_2F_2$; (b) 2% VC, 2% VC + 1% $LiPO_2F_2$, PES211 and PES211 + 1% $LiPO_2F_2$ and (c) 2% FEC, 2% FEC + 1% $LiPO_2F_2$, 1% DTD and 1% DTD + 1% $LiPO_2F_2$ after cell formation at 40. ± 0.1 °C. Panel (d) summarizes the diameter of the "semicircle" in the impedance spectra in panels a, b and c. The error bars in (d) are differences between the measurements for pair cells.

may be produced during cycling. Cells were stopped after about 350 h cycling or after the capacity loss reached 20%.

Symmetric coin cells were constructed from electrodes after dissembling some of these pouch cells. Symmetric cells have been used to distinguish the contributions of the impedance of the negative and positive electrode to the impedance of the full cells [23–25]. Detailed procedures for symmetric cell construction were described by Petibon et al. [24]. The pouch cells were charged or discharged to 3.8 V and held at 3.8 V for 1 h (approx. 50% state of charge) before they were cut open in an argon-filled glove box. Eight coin-cell size (1.54 cm^2) positive electrodes and negative electrodes were cut respectively from the pouch cell electrodes with a precision punch. Three negative/negative symmetric coin cells, three positive/positive symmetric coin cells and two positive/negative coin cells were reassembled using one polypropylene blown microfiber separator (BMF – available from 3 M Co., 0.275 mm thickness, 3.2 mg/cm^2). The electrolyte used for the symmetric cells was the same as that used in the parent pouch cell. EIS measurements on symmetric cells were made at 20.°C ± 0.1 °C or 10.°C ± 0.1 °C.

3. Results and discussion

Fig. 1 shows that $Li[Ni_{0.5}Mn_{0.3}Co_{0.2}]O_2$ (NMC532)/graphite pouch cells containing 1% $LiPO_2F_2$ outperform cells with the baseline electrolyte during storage testing at both 4.4 V (parasitic reactions at the surface of the positive electrode) and 2.5 V (parasitic reactions at the surface of the negative electrode) for 500 h at 60 °C. The voltage drop of the cells during storage is indicative of parasitic reactions – a larger voltage drop signals a greater rate of parasitic reactions. Cells containing $LiPO_2F_2$ have a smaller voltage drop during storage than the baseline cells. Fig. 1a, b and 1c show that the addition of $LiPO_2F_2$ to 1.04 mol/kg $LiPF_6$ EC:DMC (3:7) significantly reduces the rate of parasitic reactions in NMC532/graphite cells as well as the amount of gas generated during storage. The addition of $LiPO_2F_2$ also lowers cell impedance compared to cells with the baseline electrolyte and cells with $LiPO_2F_2$ have reduced impedance after storage as well (Figs. 1d and S1).

Fig. 2 shows the Nyquist plots for NMC111/graphite pouch cells with different electrolyte additives measured at 3.8 V and 10 °C after cell formation. Fig. 2a shows that adding 1% or 2% $LiPO_2F_2$ to the baseline electrolyte decreases cell impedance. This is somewhat surprising because no peak associated with reduction of $LiPO_2F_2$ on the graphite negative electrode is observed as shown in Fig. S2 in the supporting information. In order to be sure that the effects of adding $LiPO_2F_2$ to the electrolyte were not just due to additional salt, 1.2 M $LiPF_6$ in EC:EMC (3:7) was also tested for comparison with 2% $LiPO_2F_2$ added to 1.0 M $LiPF_6$ in EC:EMC (3:7) (2 wt% $LiPO_2F_2$ is equivalent to 0.16 M Li salt). Fig. 2a shows that cells with 1.2 M $LiPF_6$ in EC:EMC (3:7) have identical impedance spectra as cells with 1.0 M $LiPF_6$ in EC:EMC (3:7), suggesting that $LiPO_2F_2$ acts as an additive that modifies the SEI layers in the cell. Fig. 2b shows the addition of 2% VC increases cell impedance while the combination of 2% VC and 1% $LiPF_2O_2$ yields cells with lower impedance

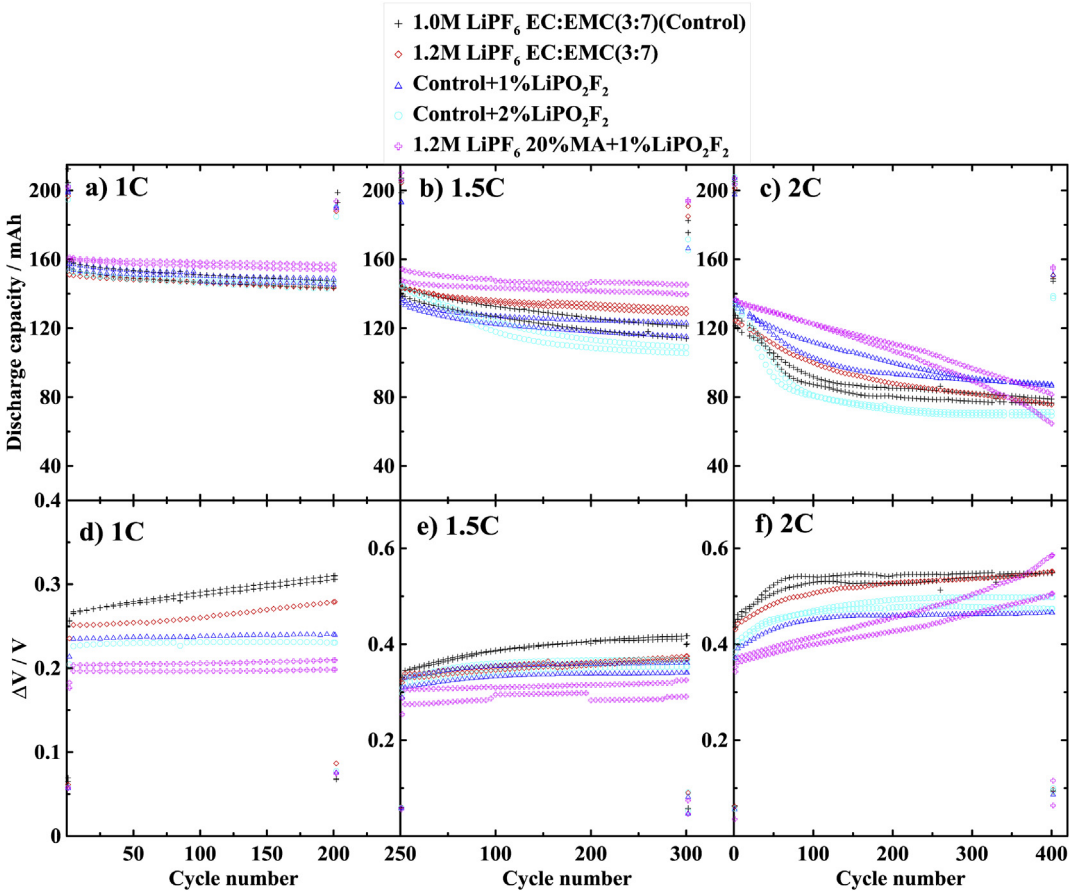

Fig. 3. (a)–(c) The discharge capacity and (d)–(f) the difference between average charge and discharge voltage (ΔV) versus cycle number for NMC111/graphite pouch cells with control, control + 1% $LiPO_2F_2$, control + 2% $LiPO_2F_2$, 1.2 M $LiPF_6$ in EC:EMC (3:7) and 1.2 M $LiPF_6$ [20% MA+ 80% EC:EMC(3:7)] + 1% $LiPO_2F_2$ cycled at 1C (a, d), 1.5C (b, e) and 2C (c, f) at 20. ± 0.1 °C. One C/20 cycle was made before and after the cycling. Results for pair cells, shown with points having the same color, were measured for every C-rate. Data points are shown for every 5th cycle. (For interpretation of the references to color in this figure legend, the reader is referred to the Web version of this article.)

relative to 2% VC. Fig. 2b shows that cells with PES211 have high impedance and that the addition of 1% $LiPO_2F_2$ to PES211 increases the diameter of the semi-circle in the Nyquist plot by 50%. Fig. 2a and b show that adding 20% methyl acetate (MA) as a co-solvent in EC:EMC (3:7) electrolyte slightly reduces cell impedance. Methyl acetate was added as a co-solvent because it increases the electrolyte conductivity (shown in Fig. S3). Fig. 2c shows that the addition of 2% FEC or 1% DTD to the baseline electrolyte reduces cell impedance while cells with 1% $LiPO_2F_2$ + 2% FEC or 1% $LiPO_2F_2$ + 1% DTD have similar impedance to cells with 2% FEC or 1% DTD alone, respectively.

Fig. 2d shows a summary of the charge-transfer resistances, R_{ct}, of NMC111/graphite pouch cells calculated from Fig. 2a–c. R_{ct} was taken to be the diameter of the semi-circle in the Nyquist plot (shown in Fig. 2a) which includes the resistances associated with ion desolvation and transport of electrons and ions through the SEIs on both the positive and negative electrodes (collectively called the charge transfer resistance, R_{ct}, here). Fig. 2d shows that 1% $LiPO_2F_2$, 2% FEC, 1% DTD and their combinations are effective impedance reducers. The use of 20% MA as a co-solvent slightly lowers cell impedance compared with EC:EMC (3:7) alone.

Since cells with 1% $LiPO_2F_2$, 2% $LiPO_2F_2$, 2% FEC, 1% DTD or the combination of 1% $LiPO_2F_2$ with 2% FEC or 1% DTD have smaller impedance, their high-rate cycling performances are expected to be better than cells containing control electrolyte. Therefore, cells with these additives were cycled at different charge rates at 20 °C. Fig. 3a–c show the discharge capacity versus cycle number for NMC111/graphite pouch cells containing 1% or 2% $LiPO_2F_2$ tested with different C-rates: 1C (3a); 1.5C (3b) and 2C (3c) during cycling to 4.1 V at 20 °C. One C/20 cycle was made before and after the cycling. As cells were cycled only up to 4.1 V at 20 °C, the capacity loss caused by electrolyte oxidation and transition metal dissolution at the cathode side is negligible [26,27]. The capacity loss due lithium inventory loss at the negative electrode should be similar at different charge rates in the absence of lithium plating for testing made at 20 °C [28]. Therefore, the rapid capacity loss during cycling at high charge rate is caused by electrolyte reduction associated with unwanted lithium plating on the graphite electrode. Fig. 3a shows that cells with control electrolyte or with the addition of 1% or 2% $LiPO_2F_2$ have nearly the same capacity retention (about 95%) and that no rapid capacity loss occurs during cycling at 1C. Fig. 3b and c show that cells with 2% $LiPO_2F_2$ have more capacity loss than control electrolyte while cells with 1% $LiPO_2F_2$ have nearly the same capacity retention as cells with control electrolyte during cycling at 1.5C and 2C, indicating 2% $LiPO_2F_2$ is not good for high-rate cycling. Fig. S3 gives a clue about why this could be the case. The conductivity of the electrolyte decreases as $LiPO_2F_2$ is added and this could be the trigger for unwanted lithium plating at 1.5 and 2C for cells with 2% $LiPO_2F_2$. Conversely, Fig. 3b shows that cells with 20% MA as co-solvent and 1% $LiPO_2F_2$ as the additive have slightly better performance compared to cells with control +1% $LiPO_2F_2$ during cycling at 1.5C probably due to the high conductivity of MA shown in Fig. S3 in the supporting information. However, cells with 20% MA have relatively fast capacity loss during 2C cycling shown in

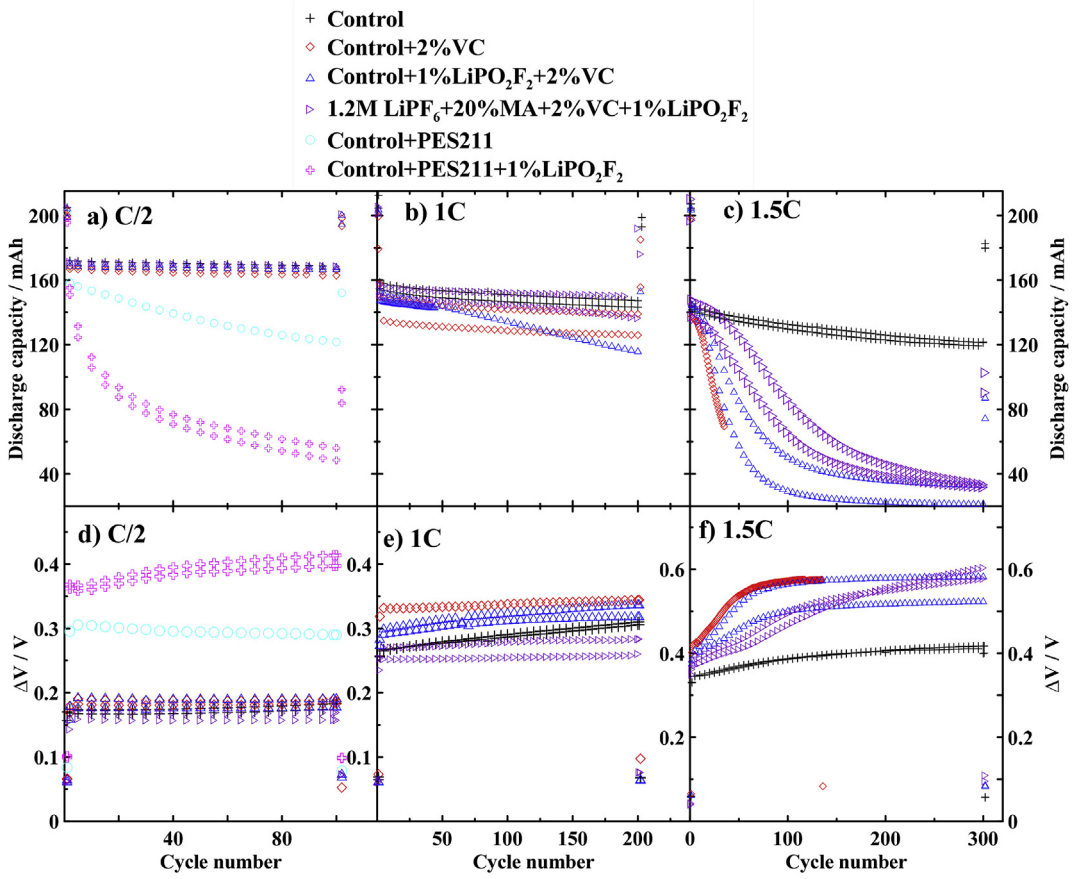

Fig. 4. (a)–(c) The discharge capacity and (d)–(f) the corresponding ΔV vs. cycle number for NMC111/graphite pouch cells cycled at C/2 (a, d), 1C (b, e) and 1.5C (c, f) at 20. ± 0.1 °C with 2% VC, 2% VC + 1% $LiPO_2F_2$, PES211 and PES211 + 1% $LiPO_2F_2$. One C/20 cycle was made before and after the cycling. Results for pair cells, shown with points having the same color, were measured for every C-rate. Data points are shown for every 5th cycle. (For interpretation of the references to color in this figure legend, the reader is referred to the Web version of this article.)

Fig. 3c perhaps because MA is not compatible with plated lithium.

Fig. 3d–f show the difference between the average charge and discharge voltage (ΔV) versus cycle number for the testing corresponding to Fig. 3a–c, respectively. The voltage difference (ΔV) is a measure of cell polarization and an increase in ΔV with cycle number indicates impedance growth during cycling, probably caused by parasitic reactions during cycling. Fig. 3d shows that ΔV increases more slowly with cycle number during 1C cycling for cells with 1% or 2% $LiPO_2F_2$ than cells with control electrolyte, suggesting that $LiPO_2F_2$ is limiting parasitic reactions between the electrolyte and the charged electrode materials in agreement with Fig. 1. Fig. 3e and f show that ΔV increases slowly with cycle number for cells with 1% or 2% $LiPO_2F_2$ even though the capacity loss for cells with 2% $LiPO_2F_2$ is much faster during cycling at 1.5C and 2C. These data indicate that 1% $LiPO_2F_2$ is enough to reduce cell impedance growth without causing rapid capacity loss. Fig. 3d, e and 3f show that cells with 20% MA as the co-solvent and 1% $LiPO_2F_2$ as the additive have the smallest ΔV and have slow ΔV growth during cycling at 1C or 1.5C while ΔV increases faster during cycling at 2C. The increased ΔV growth during 2C cycling for cells with 20% MA as the co-solvent and 1% $LiPO_2F_2$ as the additive is consistent with the rapid capacity loss shown in Fig. 3c.

Fig. 4a–c show the discharge capacity versus cycle number for NMC111/graphite pouch cells containing combinations of 2% VC or PES211 with 1% $LiPO_2F_2$ tested with different C-rates: C/2 (4a); 1C (4b) and 1.5C (4c) during cycling to 4.1 V at 20 °C. Fig. 4a shows that the combination of PES211 with 1% $LiPO_2F_2$ worsens the cycling performance at C/2 which is consistent with the higher impedance of cells with PES211 + 1% $LiPO_2F_2$ shown in Fig. 2b. The effects of the addition of 1% $LiPO_2F_2$ to PES211 will be discussed later when the impedances of symmetric cells are considered. Fig. 4a–c show that the addition of 1% $LiPO_2F_2$ to 2% VC does not improve the cycling performance at high charge rate, suggesting that the SEI on the negative electrode is still dominated by the reduction of VC when both 1% $LiPO_2F_2$ and 2% VC were added to control electrolyte. Fig. 4b and c show that cells with 20% MA as co-solvent (higher ionic conductivity) have nearly the same performance as cells with EC:EMC (3:7) solvent when 2% VC was added, indicating that cell performance at high charge rate is still dominated by the highly resistive SEI formed by VC reduction rather than the low ionic conductivity.

Fig. 4d–f show ΔV versus cycle number for the testing corresponding to Fig. 4a–c, respectively. Fig. 4d shows that cells with both 1% $LiPO_2F_2$ and PES211 have a large value of ΔV which induces high polarization and serious lithium plating even at C/2, thus the rapid capacity loss shown in Fig. 4a. Fig. 4e and f show that cells with both 1% $LiPO_2F_2$ and 2% VC have nearly the same ΔV growth as cells containing 2% VC alone during cycling. This again suggests that the SEI formed by VC is the main barrier for high-rate cycling when 2% VC was added.

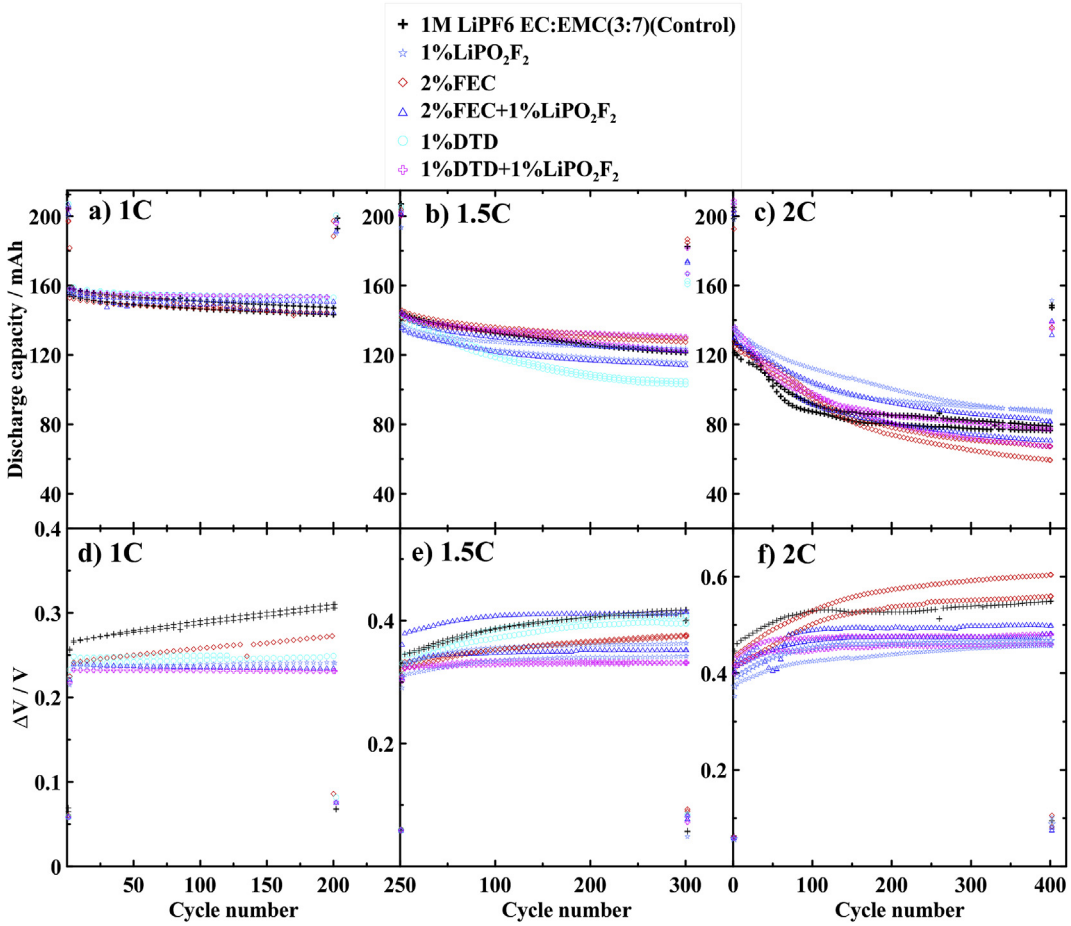

Fig. 5. (a)–(c) The discharge capacity and (d)–(f) the corresponding ΔV vs. cycle number for NMC111/graphite pouch cells cycled at 1C (a, d), 1.5C (b, e) and 2C (c, f) at 20. ± 0.1 °C with different electrolyte additive combinations: 2% FEC, 2% FEC +1% $LiPO_2F_2$, 1% DTD and 1% DTD +1% $LiPO_2F_2$. One C/20 cycle was made before and after the cycling. Results for pair cells, shown with points having the same color, were measured for every C-rate. Data points are shown for every 5th cycle. (For interpretation of the references to color in this figure legend, the reader is referred to the Web version of this article.)

Fig. 5a–c show the discharge capacity versus cycle number for NMC111/graphite pouch cells containing combinations of 2% FEC or 1% DTD with 1% $LiPO_2F_2$ tested with different C-rates: 1C (Fig. 5a); 1.5C (Fig. 5b) and 2C (Fig. 5c) during cycling between 2.8 V and 4.1 V at 20 °C. Fig. 5a shows that cells have similar capacity retention during cycling at 1C. Fig. 5b shows that cells with 1% DTD have more capacity loss during cycling at 1.5C while the addition of 1% $LiPO_2F_2$ to 1% DTD improves the cycle performance compared to cells containing 1% DTD. Fig. 5c shows that all cells with and without additives have rapid capacity loss during cycling at 2C, indicating serious lithium plating occurs at 2C regardless of the electrolyte used.

Fig. 5d–f show ΔV versus cycle number for the testing corresponding to Fig. 5a–c, respectively. Fig. 5d–f show that ΔV growth is very fast for cells with control electrolyte while the addition of 1% $LiPO_2F_2$ alone or in combination with 2% FEC or 1% DTD slows the impedance growth during cycling. This again shows that $LiPO_2F_2$ is very effective in reducing the impedance growth during cycling.

Fig. 6 shows the capacity loss measured during the C/20 cycles before and after high rate cycling at 20 °C. Pair cells were measured for each charge rate and the error bars indicate the difference between the two results. The blue dashed line in Fig. 6 is an indicator of lithium plating. Under the blue dashed line, the capacity loss is less than 5% which occurs even at small charge rates and this capacity loss is probably caused by the growth and repair of the negative electrode SEI during cycling. The larger capacity loss above the blue dashed line indicates unwanted lithium plating as lithium plating accelerates capacity loss.

Fig. 6a shows that rapid capacity loss, thus lithium plating starts from 1.5C for cells with control, control +1% $LiPO_2F_2$ and control +2% $LiPO_2F_2$. Among them, cells with 2% $LiPO_2F_2$ have the largest capacity loss during cycling at 1.5C. Fig. 6b shows that cells with 2% VC have larger capacity loss after cycling at 1.5C compared to control cells, indicating lithium plating is more prone to occur for cells with 2% VC. The combination of 2% VC with 1% $LiPO_2F_2$ has no advantages for high-rate cycling even when 20% MA was used as a co-solvent to improve the electrolyte ionic conductivity. Fig. 6c shows that compared with control electrolyte, cells with 2% FEC, 1% DTD, 2% FEC +1% $LiPO_2F_2$ or 2% FEC +1% $LiPO_2F_2$ have slightly lower capacity loss than control electrolyte during cycling at 1C, indicating the SEI formed by these additives is more protective, and less active lithium is consumed by the SEI growth or repair during cycling at 1C. However, when cells undergo 1.5C charging, all cells have rapid capacity loss (>5%) and lithium plating, especially cells with 1% DTD. Li plating at higher charge rate is confirmed by the photographs of the negative electrode after cycling at 1C and 1.5C shown in Fig. S4 in the supporting information. For example, uniform red graphite electrode (LiC_{12}) was seen after cycling at 1C in cells with control electrolyte and cells with control + 1% $LiPO_2F_2$ (Figs. S4a and c) while grey metallic Li (shown in the yellow boxes in Fig. S4) was observed on the graphite after cycling at 1.5C in cells with control electrolyte, control + 1% $LiPO_2F_2$, 2% FEC or 2% FEC + 1% $LiPO_2F_2$. The pictures of the negative electrode after cycling further confirm the rapid capacity loss in Fig. 6 is caused by lithium plating.

In order to study effects of $LiPO_2F_2$, and combinations with

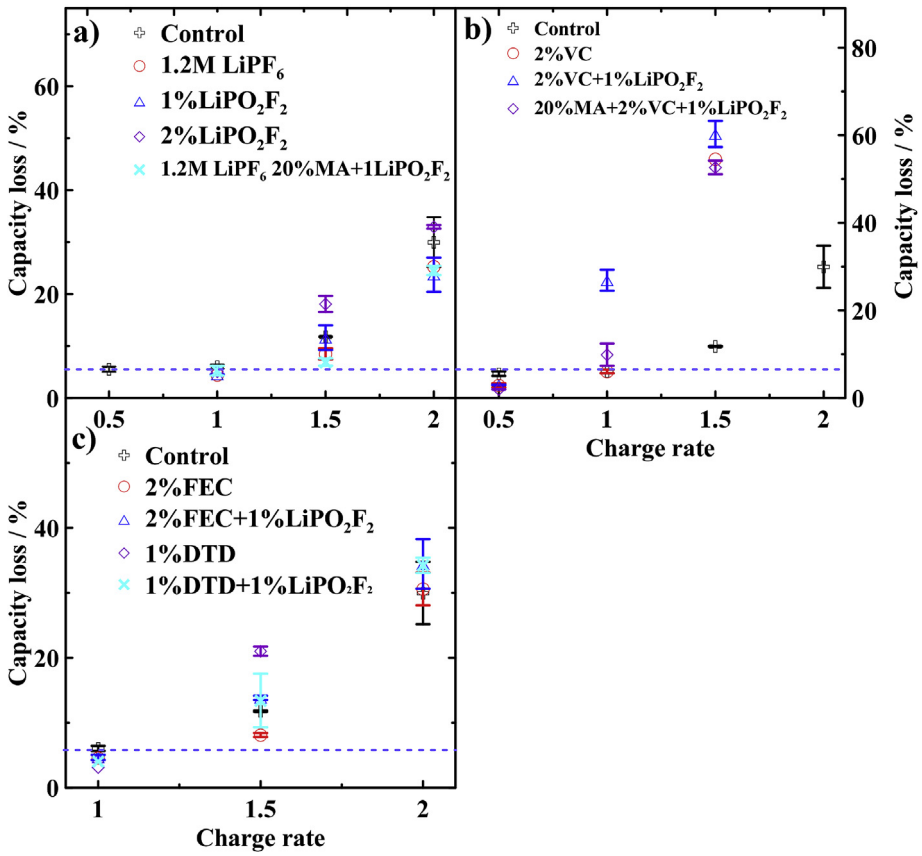

Fig. 6. The capacity loss measured from the C/20 cycles before and after the high rate cycling at 20 °C for cells with: (a) Control, 1% $LiPO_2F_2$, 2% $LiPO_2F_2$; (b) the additives 2% VC, 2% VC + 1% $LiPO_2F_2$, PES211 and PES211 + 1% $LiPO_2F_2$; (c) the additives 2% FEC, 2% FEC+1% $LiPO_2F_2$, 1% DTD and 1% DTD+ 1% $LiPO_2F_2$. The error bars are the standard deviation of data from the pair cells cycling at the same current and with the same electrolyte.

PES211, 2% FEC and 1% DTD, on the positive and negative electrode impedance separately, cells with these additives after formation were dissembled and symmetric cells were made in an argon-filled glovebox. Fig. 7 shows the area-specific Nyquist plots of the reassembled full coin cells, positive electrode symmetric cells and negative electrode symmetric cells constructed from parent NMC111/graphite pouch cells containing 1% $LiPO_2F_2$, 2% $LiPO_2F_2$, 2% FEC, 1% DTD, 2%VC, PES211 and their combinations with 1% $LiPO_2F_2$. The symmetric cells were reassembled from the parent pouch cells after formation using the same electrolyte formulation as the parent pouch cell. Fig. 7a shows that the impedance of the full coin cells decreases with the addition of $LiPO_2F_2$ which is similar to the full pouch cells shown in Fig. 2a. Fig. 7b and c show that the impedance decrease of the full cells containing 1% or 2% $LiPO_2F_2$ is due to the negative electrode. This indicates a less resistive SEI on the negative electrode due to the presence of $LiPO_2F_2$. Fig. 7d–f show that adding 1% $LiPO_2F_2$ to 2% FEC or 1% DTD has little impact on the impedance of both the positive and negative electrode. Fig. 7g–i show that the addition of 1% $LiPO_2F_2$ to PES211 increases cell impedance primarily due to impedance increase of the negative electrode. This indicates that $LiPO_2F_2$ participates in SEI formation and the interaction of $LiPO_2F_2$ with PES211 promotes a highly resistive SEI on the negative electrode.

Fig. 8a shows $R_{negative}$ for cells with different electrolytes obtained from the Nyquist plots of the negative/negative symmetric cells shown in Fig. 7c,f and g. Here, $R_{negative}$ includes the processes of ion desolvation, electron and ion transport through the SEI (collectively called charge transfer resistance here) and current collector/active particle contact resistance of the negative electrode (small high frequency shoulder in the EIS spectra) [29,30]. Fig. 7c,f

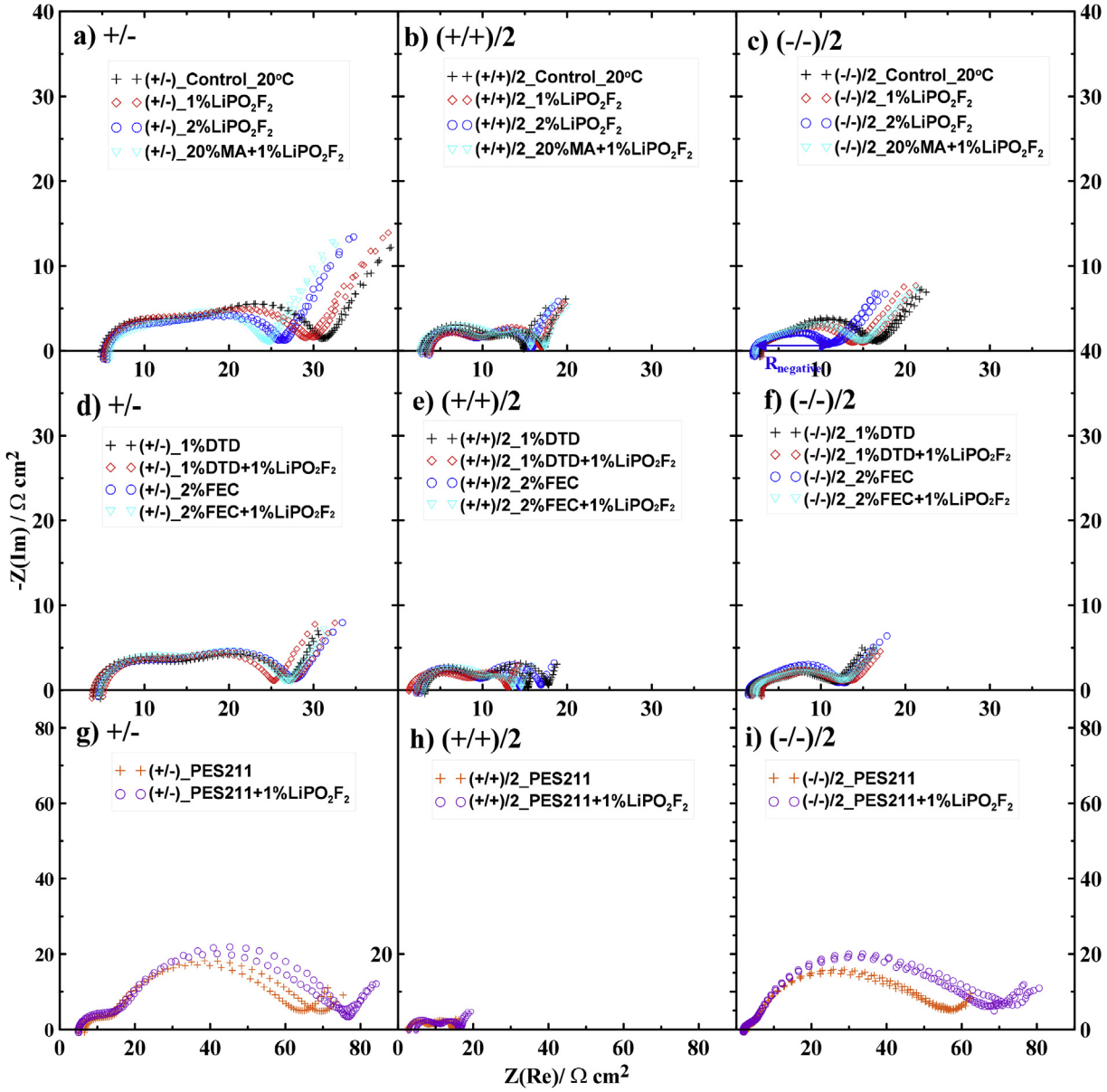

Fig. 7. The area-specific Nyquist plots of full reassembled coin cells (a, d, g), the positive symmetric cell impedance divided by two (b, e, h) and the negative symmetric cell impedance divided by two (c, f, i) for cells containing control electrolyte, 1%, 2% $LiPO_2F_2$ (a, b, c), 2% FEC, 2% FEC + 1% $LiPO_2F_2$, 1% DTD and 1% DTD + 1% $LiPO_2F_2$ (d, e, f), and 2% VC, PES211 and PES211 + 1% $LiPO_2F_2$ (g, h, i). The electrodes used in these coin cells were extracted from NMC111/graphite pouch cells after cell formation. All EIS measurements were made at 20 °C.

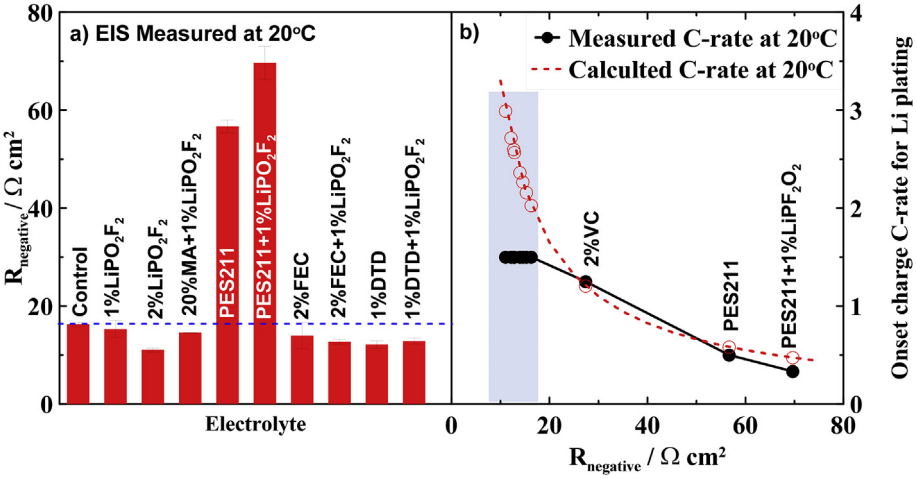

Fig. 8. a) The diameter of the "semicircle" ($R_{negative}$) in the impedance spectra shown in Fig. 7c, f and 7i. The error bars are differences in the measurements for three "brother" symmetric negative/negative coin cells. b) The measured onset current (the black line/scatter) for unwanted lithium plating for cells with different electrolytes during cycling at 20 °C as well as the predictions (the red dashed line) calculated from $R_{negative}$ in a). $R_{negative}$ is less than 20 Ω × cm^2 in b) for cells with control, 20% MA + 1% $LiPO_2F_2$, 2% FEC, 2% FEC +1% $LiPO_2F_2$, 1% DTD +1% $LiPO_2F_2$, 1% DTD, 2% $LiPO_2F_2$ from highest (control) to lowest (2% $LiPO_2F_2$). (For interpretation of the references to color in this figure legend, the reader is referred to the Web version of this article.)

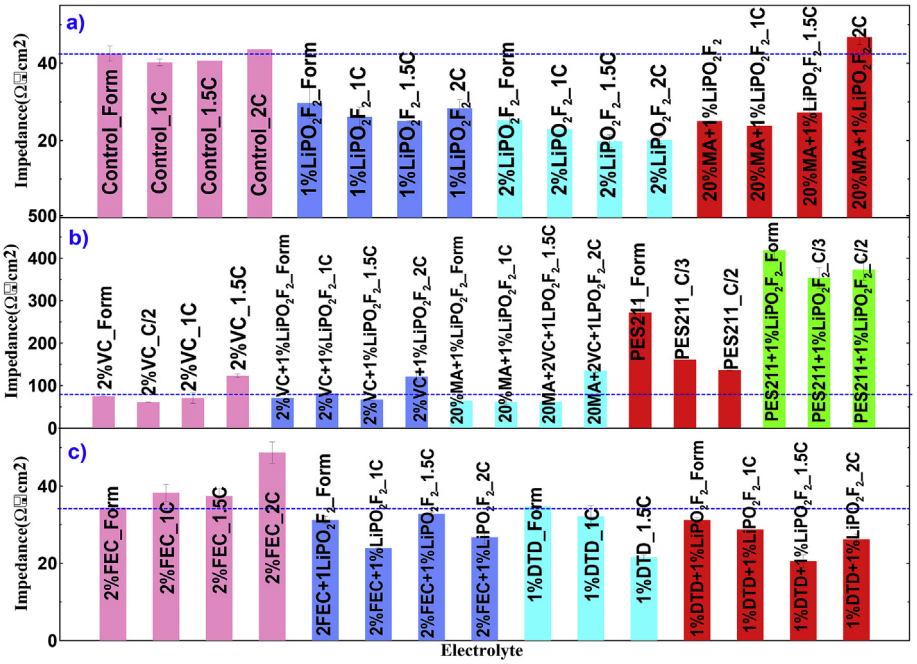

Fig. 9. The diameter of the semicircle in the EIS spectra for NMC111/graphite pouch cells, after cell formation and after 20 °C cycling at C/3, C/2, 1C, 1.5C and 2C for cells containing: (a) control, control + 1% $LiPO_2F_2$, control + 2% $LiPO_2F_2$, 1.2 M $LiPF_6$ in EC:EMC (3:7) and 1.2 M $LiPF_6$ in [20% MA+ 80% EC:EMC (3:7)] + 1% $LiPO_2F_2$; (b) 2% VC, 2% VC + 1% $LiPO_2F_2$, PES211 and PES211 + 1% $LiPO_2F_2$ and (c) 2% FEC, 2% FEC + 1% $LiPO_2F_2$, 1% DTD and 1% DTD + 1% $LiPO_2F_2$.

and i show that the charge transfer resistance (the diameter of mid-frequency semi-circle) is the main component of $R_{negative}$ [30] which means that the charge transfer resistance of the negative electrode dominates the changes in $R_{negative}$. Fig. 8a clearly shows that adding 2% $LiPO_2F_2$ to control electrolyte yields cells with the lowest $R_{negative}$ while the combination of PES211 with $LiPO_2F_2$ increases $R_{negative}$ relative to PES211. Though adding 1% $LiPO_2F_2$ to 2% FEC or 1% DTD has little impact on $R_{negative}$, 2% FEC, 1% DTD and combinations of FEC or DTD with $LiPO_2F_2$ reduce $R_{negative}$ compared to cells with control electrolyte.

As discussed in our previous work [9] the onset current for unwanted lithium plating (I_u) can be well predicted by the expression: $I_u = 0.080\ V \times S/R_{negative}$, where 0.080 V is the over-potential needed for lithium plating, S is the geometric electrode surface area in a full cell and $R_{negative}$ is the area specific negative electrode resistance obtained from negative/negative symmetric cells. The prediction of this simple rule-of-thumb relation agrees well with the trends observed in experiment under conditions where $R_{negative}$ is the dominant factor for anode polarization [9]. Fig. 8b shows a comparison between the calculated onset C-rate for lithium plating using the expression: $I_u = 0.080\ V \times S/R_{negative}$ and the measured results. The measured C-rate for lithium plating was

obtained from the onset of rapid capacity loss shown in Fig. 6 and the post-mortem analysis shown in Fig. S4. Fig. 8b shows that the measured results for cells with 2% VC, PES211 and PES211 + 1% $LiPO_2F_2$ agree well with the calculated results. However, when $R_{negative}$ is lower than $20\,\Omega \times cm^2$ for the graphite electrode we used, there is a large difference between the measured results and the calculated results. As $R_{negative}$ decreases, unwanted lithium plating still occurs at about 1.5C for cells with various additives rather than at the higher charge C-rate calculated. This suggests that when the charge transfer resistance is low enough ($20\,\Omega \times cm^2$), overpotentials due to other factors such as lithium diffusion in the graphite and lithium-ion diffusion in the electrolyte become the dominant factors for lithium plating which have not been considered in the simple model. This is consistent with results of Ji et al., who reported that Li diffusion in electrolyte and Li diffusivity in graphite particles are rate-determining factors of Li-ion cells during discharge at −20 °C and 1C through modeling [31]. Fig. 8b also shows that additives that could reduce the charge transfer resistance cannot prevent unwanted lithium plating when the charge transfer resistance is too small to be the dominant factor. The size of the active artificial graphite particles was 15–30 μm in our cells. Cells with smaller graphite particles will tolerate higher charges rate when the charge transfer resistance is small.

It is very important to stress the importance of the results in Fig. 8. The calculated curve in Fig. 8 shows the clear value of using $LiPO_2F_2$ as an additive to improve high rate charging. Cells with thinner electrodes, increased porosity and smaller graphite particles than used in the cells in this report will certainly benefit from the use of $LiPO_2F_2$. It is hoped that producers of Li-ion power cells will explore the impact of $LiPO_2F_2$ additions in their cells.

Fig. 9a, b and c show the charge transfer resistance, R_{ct}, (diameter of the semi-circle in the Nyquist plot) after formation and after 20 °C cycling at C/2, 1C and 1.5C for pouch cells containing (9a) control, 1% $LiPO_2F_2$ and 2% $LiPO_2F_2$; (9b) 2% VC, 2% VC + 1% $LiPO_2F_2$, PES211 and PES211 + 1% $LiPO_2F_2$ and (9c) 2% FEC, 2% FEC + 1% $LiPO_2F_2$, 1% DTD, 1% DTD + 1% $LiPO_2F_2$. The impedance spectra were measured at 3.8 V and at 10.0 °C in all cases. The complete impedance spectra for all the NMC111/graphite pouch cells are given in Figs. S5–S7 in the supporting information and R_{ct} is shown in Table S1. Fig. 9a shows that the impedance of cells with control and 20% MA +1% $LiPO_2F_2$ decreases with C-rate except for cells after 2C cycling. The increased impedance of cells after 2C cycling is probably due to large amounts of plated lithium on the negative electrode and possibly due to a lower state of charge at 3.8 V for aged cells. Fig. 9b shows that cells with 2% VC with and without 1% $LiPO_2F_2$ have a similar trend to the control cells in Fig. 9a. That is, cell impedance decreases with charge C-rate except at 1.5C. Figs. 9a and c show that cells containing 1% $LiPO_2F_2$, 2% $LiPO_2F_2$, 1% $LiPO_2F_2$ + 2% FEC and 1% $LiPO_2F_2$ + 1% DTD have much smaller impedance even after cycling at 2C. This is in agreement with the lower growth rate of ΔV during high rate cycling shown in Figs. 3 and 5.

In order to analyze the reasons for the slow ΔV and impedance growth during cycling at high charge rate for cells with $LiPO_2F_2$, symmetric cells fabricated using electrodes from parent pouch cells after cycling at 1.5C were studied using EIS. EIS measurements for positive and negative electrode symmetric cells can determine which electrode contributed most to impedance changes during

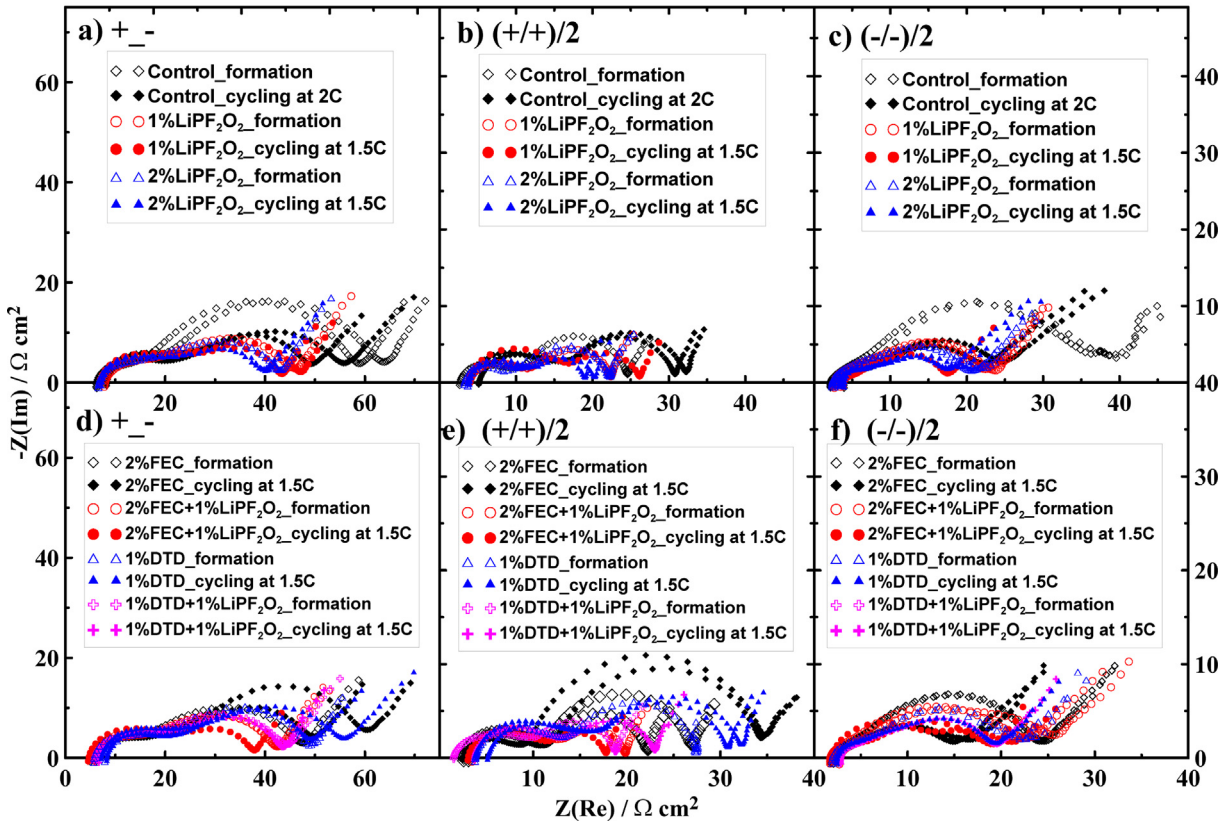

Fig. 10. The area-specific Nyquist plots of reassembled full coin cells (a, d), the positive/positive symmetric coin cells divided by two (b, e) and the negative/negative symmetric coin cells divided by two (c, f) for cells containing control, 1% $LiPO_2F_2$ and 2% $LiPO_2F_2$ (a, b, c), and 2% FEC, 2% FEC + 1% $LiPO_2F_2$, 1% DTD and 1% DTD + 1% $LiPO_2F_2$ (d, e, f). The electrodes used in these coin cells were extracted from NMC111/graphite pouch cells after formation and after cycling at 1.5C in Fig. 2b and 4b, respectively. All EIS measurements were made at 10 °C.

cycling. Fig. 10a shows that the impedance spectra of the full coin cells decreases slightly after cycling at 1.5C for cells with control, 1% $LiPO_2F_2$ and 2% $LiPO_2F_2$. Fig. 10b shows that the positive electrode impedance increases for cells with control electrolyte after cycling while the positive electrode impedance shows a slight decrease for cells with 1% and 2% $LiPO_2F_2$ after cycling. Fig. 10c shows the impedances of all the negative electrode symmetric cells decreases slightly during cycling, especially cells with control electrolyte. Similar to control electrolyte, Fig. 10d–f show that in cells with 2% FEC or 1% DTD, the negative electrode impedance is lower while the positive electrode impedance is higher after cycling. When 1% $LiPO_2F_2$ is added to 2% FEC, the behavior is changed: both the negative and positive electrode impedance is lower after cycling. In short, adding 1% $LiPO_2F_2$ inhibits positive electrode impedance increase during cycling. This reduction of the positive electrode impedance is probably the reason that $LiPO_2F_2$ slows impedance growth during cycling.

4. Conclusions

The impacts of $LiPO_2F_2$ alone and in combination with 2% VC, PES211, 2% FEC and 1% DTD on unwanted lithium plating were studied in NMC111/graphite pouch cells. The work showed that 1% $LiPO_2F_2$ alone is a promising additive for reducing cell impedance. The behavior of $LiPO_2F_2$ depends on the presence of other additives. When 1% $LiPO_2F_2$ was combined with 1% DTD or 2% FEC, impedance growth during cycling was highly suppressed although the cycle performance was not improved for the cells used here. However, when 1% $LiPO_2F_2$ was added to PES211, cell impedance increased, thus unwanted lithium plating occurred at lower charge rate. This suggests that not all additive combinations have benefits and the combination of electrolyte additives should be well chosen.

EIS measurements on symmetric cells made from parent cells after formation showed that the addition of $LiPO_2F_2$ decreased the resistance of the negative electrode which should raise the onset current for unwanted lithium plating. However, the high rate cycling performance of cells with 1% $LiPO_2F_2$ was not improved and cells with 2% $LiPO_2F_2$ had worse performance during cycling at 1.5C and 2C. This suggested that other factors dominated the high-rate charging behavior when the charge transfer resistance of the negative electrode was small enough. Nevertheless, it is strongly believed that $LiPO_2F_2$ can improve the high rate charging behavior of Li-ion cells designed for high power, when the limiting factor is presently the negative electrode SEI resistance.

EIS measurements on symmetric cells made from parent pouch cells after formation and cycling showed that the positive electrode impedance increased after cycling for cells with control electrolyte, 2% FEC and 1% DTD. When 1% $LiPO_2F_2$ was added to control electrolyte and to electrolyte with 2% FEC, the impedance growth of the positive electrode during cycling was reduced. This is probably the reason for slow ΔV growth during cycling and low impedance after cycling. The effects of $LiPO_2F_2$ on the positive and negative electrode impedance after formation and after cycling deserve further studies using surface science tools.

$LiPO_2F_2$ is a promising electrolyte additive for reducing impedance growth during high-rate cycling. Additionally, cells with 1% $LiPO_2F_2$ have outstanding storage performance at 60 °C. The impact of $LiPO_2F_2$, in combination with other additives, on long term Li-ion cell lifetime should be well studied.

Acknowledgements

The authors thank NSERC, 3M Canada and Tesla Motors for the funding of this work under the auspices of the Industrial Chairs program. Qianqian Liu acknowledges the generous support of the China Scholarship Council. The authors thank Shenzhen Capchem Technology Co. and Guangzhou Tinci new Materials Technology Co. for the $LiPO_2F_2$ used in this work. The authors thank Dr. Jing Li of BASF for the solvents and traditional additive used in this work.

Appendix A. Supplementary data

Supplementary data related to this article can be found at https://doi.org/10.1016/j.electacta.2018.01.058.

References

[1] J. Vetter, P. Novák, M.R. Wagner, C. Veit, K.C. Möller, J.O. Besenhard, M. Winter, M. Wohlfahrt-Mehrens, C. Vogler, A. Hammouche, Ageing mechanisms in lithium-ion batteries, J. Power Sources 147 (2005) 269–281.
[2] Z. Li, J. Huang, B. Yann Liaw, V. Metzler, J. Zhang, A review of lithium deposition in lithium-ion and lithium metal secondary batteries, J. Power Sources 254 (2014) 168–182.
[3] Q.Q. Liu, C.Y. Du, B. Shen, P.J. Zuo, X.Q. Cheng, Y. Ma, G.P. Yin, Y.Z. Gao, Understanding undesirable anode lithium plating issues in lithium-ion batteries, RSC Adv. 6 (2016) 88683–88700.
[4] V. Zinth, C. von Lüders, M. Hofmann, J. Hattendorff, I. Buchberger, S. Erhard, R. Gilles, Lithium plating in lithium-ion batteries at sub-ambient temperatures investigated by in situ neutron diffraction, J. Power Sources 271 (2014) 152–159.
[5] K.G. Gallagher, S.E. Trask, C. Bauer, T. Woehrle, S.F. Lux, M. Tschech, P. Lamp, B.J. Polzin, S. Ha, B. Long, Q. Wu, Optimizing areal capacities through understanding the limitations of lithium-ion electrodes, J. Electrochem. Soc. 163 (2016) A138–A149.
[6] J. Fan, S. Tan, Studies on charging lithium-ion cells at low temperatures, J. Electrochem. Soc. 153 (2006) A1081–A1092.
[7] H. Buqa, D. Goers, M. Holzapfel, M.E. Spahr, P. Novák, High rate capability of graphite negative electrodes for lithium-ion batteries, J. Electrochem. Soc. 152 (2005) A474–A481.
[8] J.-P. Jones, M.C. Smart, F.C. Krause, B.V. Ratnakumar, E.J. Brandon, The effect of electrolyte composition on lithium plating during low temperature charging of Li-Ion cells, ECS Trans. 75 (2017) 1–11.
[9] Q.Q. Liu, R. Petibon, C.Y. Du, J.R. Dahn, Effects of electrolyte additives and solvents on unwanted lithium plating in lithium-ion cells, J. Electrochem. Soc. 164 (2017) A1173–A1183.
[10] G. Yang, J. Shi, C. Shen, S. Wang, L. Xia, H. Hu, Z. Liu, Improving the cyclability performance of lithium-ion batteries by introducing lithium difluorophosphate ($LiPO_2F_2$) additive, RSC Adv. 7 (2017) 26052–26059.
[11] B. Yang, H. Zhang, L. Yu, W. Fan, D. Huang, Lithium difluorophosphate as an additive to improve the low temperature performance of $LiNi_{0.5}Co_{0.2}Mn_{0.3}O_2$/graphite cells, Electrochim. Acta 221 (2016) 107–114.
[12] K.-E. Kim, J.Y. Jang, I. Park, M.H. Woo, M.H. Jeong, W.C. Shin, M. Ue, N.S. Choi, A combination of lithium difluorophosphate and vinylene carbonate as reducible additives to improve cycling performance of graphite electrodes at high rates, Electrochem. Commun. 61 (2015) 121–124.
[13] A. Sano, S. Maruyama, Decreasing the initial irreversible capacity loss by addition of cyclic sulfate as electrolyte additives, J. Power Sources 192 (2009) 714–718.
[14] X. Li, Z. Yin, X. Li, C. Wang, Ethylene sulfate as film formation additive to improve the compatibility of graphite electrode for lithium-ion battery, Ionics 20 (2014) 795–801.
[15] Z. Ding, X. Li, T. Wei, Z. Yin, X. Li, Improved compatibility of graphite anode for lithium ion battery using sulfuric esters, Electrochim. Acta 196 (2016) 622–628.
[16] R. McMillan, H. Slegr, Z.X. Shu, W.D. Wang, Fluoroethylene carbonate electrolyte and its use in lithium ion batteries with graphite anodes, J. Power Sources 81 (1999) 20–26.
[17] L. Liao, P. Zuo, Y. Ma, Y. An, G. Yin, Y. Gao, Effects of fluoroethylene carbonate on low temperature performance of mesocarbon microbeads anode, Electrochim. Acta 74 (2012) 260–266.
[18] T. Sasaki, T. Abe, Y. Iriyama, M. Inaba, Z. Ogumi, Suppression of an alkyl dicarbonate formation in Li-ion cells, J. Electrochem. Soc. 152 (2005) A2046–A2050.
[19] D. Aurbach, K. Gamolsky, B. Markovsky, Y. Gofer, M. Schmidt, U. Heider, D. Aurbach, K. Gamolsky, B. Markovsky, et al., On the use of vinylene carbonate (VC) as an additive to electrolyte solutions for Li-ion batteries, Electrochim. Acta 47 (2002) 1423–1439.
[20] J. Li, H.Y. Li, A. Cameron, S. Glazier, Q.Q. Liu, J.R. Dahn, Impact of electrolyte additive content on the lifetime of $LiNi_{0.5}Mn_{0.3}Co_{0.2}O_2$/artificial and natural graphite cells, J. Electrochem. Soc. 164 (2017) A2756–A2766.
[21] K.J. Nelson, G.L. d'Eon, A.T.B. Wright, L. Ma, J. Xia, J.R. Dahn, Studies of the effect of high voltage on the impedance and cycling performance of Li $[Ni_{0.4}Mn_{0.4}Co_{0.2}]O_2$/Graphite lithium-ion pouch cells, J. Electrochem. Soc. 162 (2015) A1046–A1054.
[22] B. Gyenes, D.A. Stevens, V.L. Chevrier, J.R. Dahn, Understanding anomalous behavior in coulombic efficiency measurements on Li-ion batteries,

J. Electrochem. Soc. 162 (2015) A278–A283.
[23] J.C. Burns, R. Petibon, K.J. Nelson, N.N. Sinha, A. Kassam, B.M. Way, J.R. Dahn, Studies of the effect of varying vinylene carbonate (VC) content in lithium ion cells on cycling performance and cell impedance, J. Electrochem. Soc. 160 (2013) A1668–A1674.
[24] R. Petibon, C.P. Aiken, N.N. Sinha, J.C. Burns, H. Ye, C.M. VanElzen, G. Jain, S. Trussler, J.R. Dahn, Study of electrolyte additives using electrochemical impedance spectroscopy on symmetric cells, J. Electrochem. Soc. 160 (2013) A117–A124.
[25] C.H. Chen, J. Liu, K. Amine, Symmetric cell approach and impedance spectroscopy of high power lithium-ion batteries, J. Power Sources 96 (2001) 321–328.
[26] Z. Lu, L.Y. Beaulieu, R.A. Donaberger, C.L. Thomas, J.R. Dahn, Synthesis, structure, and electrochemical behavior of $Li[Ni_xLi_{1/3-\ 2x/3}Mn_{2/3-\ x/3}]O_2$, J. Electrochem. Soc. 149 (2002) A778–A791.
[27] V. Etacheri, R. Marom, R. Elazari, G. Salitra, D. Aurbach, Challenges in the development of advanced Li-ion batteries: a review, Energy Environ. Sci. 4 (2011) 3243–3262.
[28] J. Wang, J. Purewal, P. Liu, J. Hicks-Garner, S. Soukazian, E. Sherman, A. Sorenson, L. Vu, H. Tataria, M.W. Verbrugge, Degradation of lithium ion batteries employing graphite negatives and nickel–cobalt–manganese oxide+ spinel manganese oxide positives: Part 1, aging mechanisms and life estimation, J. Power Sources 269 (2014) 937–948.
[29] M. Gaberscek, J. Moskon, B. Erjavec, R. Dominko, J. Jamnik, The importance of interphase contacts in Li ion electrodes: the meaning of the high-frequency impedance arc, Electrochem. Solid State Lett. 11 (2008) A170–A174.
[30] G.-Y. Kim, R. Petibon, J.R. Dahn, Effects of succinonitrile (SN) as an electrolyte additive on the impedance of $LiCoO_2$/graphite pouch cells during cycling, J. Electrochem. Soc. 161 (2014) A506–A512.
[31] Y. Ji, Y. Zhang, C.-Y. Wang, Li-ion cell operation at low temperatures, J. Electrochem. Soc. 160 (2013) A636–A649.